Journal name: Ecology

Manuscript type: Article

Manuscript title: Algal assemblage drives patterns in ecosystem structure but not metabolism in a productive river

Author names: Alice M. Carter[1], Robert O. Hall, Jr.[1], Rafael Feijó de Lima[2], Michael DeGrandpre[3], Qipei Shangguan[3,4], H Maurice Valett[2]

Author affiliations:

[1]Flathead Lake Biological Station, University of Montana, Polson, MT, USA

[2]Divison of Biological Sciences, University of Montana, Missoula, MT, USA

[3]Department of Chemistry, University of Montana, Missoula, MT, USA

[4]Woods Hole Oceanographic Institution, Falmouth, MA, USA

Corresponding Author: Alice M. Carter, email: alice.carter@flbs.umt.edu

Open Research Statement: The raw data presented in this manuscript are archived in a public EDI repository (Valett et al. 2023a, https://doi.org/10.6073/pasta/f24a105ec10af98edc7c9314b703e4fc). Derived data and novel code used to analyze the data and make the figures in this manuscript are publicly available in an open source zenodo repository (DOI:10.5281/zenodo.11626529).

Keywords: Algae, Metabolism, Productivity, Biomass, Aquatic, Carbon

Abstract

Although rivers tend to be heterotrophic and have low standing stocks of autotrophic biomass, algal dynamics are fundamental drivers of ecosystem processes. Filamentous algae can cause nuisance algal blooms that alter the structure of the autotrophic assemblage but their influence on ecosystem process can be more variable. Here, we examined the structural and functional contribution of filamentous and epilithic algae by linking algal biomass measurements to daily primary production fluxes throughout two growing seasons in 6 sites along the Upper Clark Fork River, an open canopy, snow melt river in western Montana, USA. We partitioned daily productivity estimates across different algal groups using the spatial and temporal variability in algal assemblages across our six sites. By using reach-scale metabolism estimates, we assessed the *in situ* functional rates of individual algal groups. Throughout two growing seasons, we measured high rates of ecosystem productivity and spatially variable filamentous algal blooms. We found that the filamentous algal blooms determined the ecosystem structure in terms of total biomass and algal turnover times, but not the ecosystem functions of gross primary productivity, ecosystem respiration, or net production. Whole-reach estimates of epilithic and filamentous algae production rates were 0.24 and 0.05 d^{-1} respectively, which are similar to rates measured in mesocosms and cultures. The epilithic algae grew and turned over rapidly, dominating total biomass production and driving ecosystem function while filamentous algae grew slowly and built up large amounts of biomass during a growing season, shaping the structure, but not function, of the ecosystem.

1 Introduction

Autotrophic assemblages shape ecosystem processes. In terrestrial ecosystems the autotrophic assemblage is the defining characteristic of the biome (e.g. grassland, deciduous forest), and vegetation's role in driving ecosystem function is well known (Whittaker, 1975). Autotrophs make up most of the biomass in terrestrial ecosystems and are major structural components, altering local environments and creating distinct habitats for animals in addition to serving as their

major food source (Aber and Melillo, 2001). By contrast, autotrophic biomass tends to be low in aquatic ecosystems (Del Giorgio et al., 1999; Odum, 1957; Vadeboncoeur and Power, 2017). Because of their intimate association with terrestrial inputs of organic matter, and shading from riparian vegetation (Fisher and Likens, 1973; Savoy et al., 2021), most streams and rivers are heterotrophic ecosystems (Bernhardt et al., 2022; Webster and Meyer, 1997), but autotrophic production of organic matter can still contribute to the energy economy of these ecosystems (Thorp and Delong, 2002; Finlay, 2001) and in appropriate conditions be the dominant source of habitat and food for riverine animals (Minshall, 1978; Uehlinger and Naegeli, 1998). While there is a long history of studying algae in streams (Patrick, 1949; Stevenson et al., 1996), there is still no strong framework connecting autotrophic communities to ecosystem metabolic fluxes.

More autotrophic biomass is often associated with greater productivity, but in streams and rivers these relationships are not consistent. Across streams within a river network, Rodríguez-Castillo et al. (2019) observed more algal biomass in reaches with higher productivity. This positive relationship occurs to a lesser extent across streams with different land uses in their watersheds (Bernot et al., 2010) but the relationships aren't strong in either case. Other times, there is no pattern linking biomass and productivity across sites (Izagirre et al., 2008) or the relationship is even inverted (Davis et al., 2012). Within many rivers algal biomass is greatest during the time of year with peak productivity (Beaulieu et al., 2013). However, it is also common for algal biomass to show little seasonality after an initial green up period even when productivity is maximal during a specific season (Roberts et al., 2007; Rosemond, 1994).

Few studies link ecosystem metabolic fluxes to primary producer types or quantities in lotic ecosystems. In terrestrial ecosystems, autotrophic abundance and plant traits are directly related to ecosystem fluxes like respiration and both gross and net primary production (Reichstein et al., 2014). In rivers and streams, variation in physiognomy (i.e., physical architecture) of the algal assemblage covaries with the diversity of benthic macroinvertebrates (Tonkin et al., 2014). However, the link between algal assemblage structure and the magnitude of primary productivity is less clear. Primary productivity declined alongside decreased primary producer biomass that

accompanied a shift from filamentous algal mats to thin periphyton biofilms in a river released from nutrient and organic matter pollution (Arroita et al., 2019). In the Loire river, a state change from a phytoplankton to a high-biomass macrophyte-dominated autotrophic assemblage showed no change in the magnitude of metabolic fluxes (Diamond et al., 2022).

Shifts in periphyton assemblages toward more filamentous algae, often in the form of nuisance algal blooms, is a growing concern for streams and rivers (Dodds and Welch, 2000; Vadeboncoeur et al., 2021; Suplee et al., 2009). Compared to thin epilithic biofilms, filamentous algal mats are particularly grazer resistant and are of low quality as a food source for stream animals (Vadeboncoeur and Power, 2017). These mats can alter the physical structure of the ecosystem, serving as habitat for stream macroinvertebrates (Furey et al., 2012) and increasing the residence time of flowing water, potentially enough to allow for localized recycling of nutrients (Mulholland et al., 1994). While filamentous mats are structurally large, often only a fraction of the mats are photosynthetically active (Higgins et al., 2006). Linking their biomass to metabolic rates can be difficult, confounding efforts to address their effects on ecosystem function.

Despite the apparent lack of a clear relationship between autotrophic biomass and productivity, its existence is often presumed by investigators addressing lotic energetics. Models often incorporate a positive relationship between biomass and production (Demars et al., 2023; Blaszczak et al., 2023), or assume that well understood properties of algal physiology such as P-I curves (Jassby and Platt, 1976) scale appropriately to entire ecosystems (Beaulieu et al., 2013). As measurements of ecosystem metabolism rapidly expand due to automation and the relative ease of data collection (Rode et al., 2016; Jankowski et al., 2021), we may see even greater reliance on tenuous relationships between production and biomass to further the assessment of stream carbon dynamics. While measurements of algal biomass are relatively straightforward, collection and analysis are labor intensive and untenable at large scales. As a result, recent extensive surveys of riverine primary production lack biomass data obtained at proper spatial or temporal scale to allow comparison between structure and function (Bernhardt et al., 2022).

Here, we use the spatial and temporal dynamics of benthic algae in the Upper Clark Fork River

(UCFR) to quantify the relationships between algal biomass and primary productivity at the reach scale. The UCFR is a mid-order, open-canopied river in western Montana, USA, that is scoured annually by snowmelt runoff followed by a growing season characterized by well-lit warm waters that support substantial benthic algal communities throughout the river's 200 km (Valett et al., 2023b). Epilithic algal assemblages of diatoms and adnate green algae are common and growing season algal blooms of the filamentous green alga, *Cladophora*, can be extensive with chlorophyll *a* standing crops exceeding 600 mg/m^2 (Suplee et al., 2012; Valett et al., 2023b). However, due in part to variation in the intensity of scour, the location and magnitude of the algal blooms varies annually and blooms are often absent from any given site during any given year. Valett et al. (2023b) characterized the temporal succession of benthic algae during snowmelt recession in the UCFR distinguishing epilithic biofilms from macroalgal filamentous green forms as distinct periphyton morphotypes that alternatively dominate algal biomass.

We linked algal biomass measurements to daily primary production fluxes throughout two growing seasons in 6 sites along the UCFR to ask: 1) What are the metabolic and algal biomass dynamics during the growing season in a highly productive, snowmelt-fed river? 2) How do filamentous algal blooms affect ecosystem structure and function? 3) What are the relative production and turnover rates of epilithic and filamentous algae in this river? To address these questions, we used estimates of reach-scale productivity and respiration to derive daily rates of autotrophic respiration and net biomass production at each site and partitioned the daily productivity between epilithic and filamentous algae using a linear model. Results illustrate that despite their ubiquitous abundance during blooms, filamentous mats contribute relatively little to stream metabolism compared to less abundant but more active epilithic biofilms.

2 Methods

2.1 Study Site

The UCFR is an open canopy cobble bed river that suffers from anthropogenic nitrogen (N) enrichment. Excess N, coupled with naturally high levels of geogenic phosphorus (P) availability

and solar insolation, leads to annual nuisance blooms of filamentous algae (*Cladophora glomerata*) (Flynn and Chapra, 2020) during summer periods of enhanced net primary productivity (Dodds et al., 1997; Suplee et al., 2012; Valett et al., 2023b). In addition to nutrient pollution, the UCFR has extensive heavy metal contamination of the river bed and floodplain due to a history of mining in the headwaters (Moore and Luoma, 1990).

During the growing seasons of 2020 and 2021, we measured algal biomass and ecosystem metabolism at six sites distributed over 200 km of the UCFR (Figure 1). At each metabolism study site, we measured upstream average reach depth at a minimum of 3 (up to 8 at some sites) different discharges by taking 10 - 15 transects of depth measurements in the 1-km reach upstream of each sensor location. We then fit a fixed slope, variable intercept model of log(depth) as a function of log(discharge), allowing sites with fewer measurements to borrow strength from those with more to create more robust relationships across sites (SI Figure 1).

2.2 Algal Biomass Sampling

During the growing seasons of 2020 and 2021, we estimated algal biomass at all sites. For both years, we collected samples every other week beginning after the spring flood had receded (13 July 2020; 22 June 2021) and continuing until mid-October. On each sampling date, we obtained 5 samples of benthic algae per site using a cylindrical benthic sampler (area = 0.08 m^2). We examined all cobbles in the sample, and, when filamentous algae were present, we removed them from the rock surfaces. We then scrubbed rocks to remove adnate forms of algal biomass (epilithic biofilms) using a brush. We kept filamentous and epilithic biofilm samples in separate cool and dark conditions, processing them in the laboratory within 24 h of collection.

In the laboratory, we filtered aqueous samples of epilithon through pre-weighed Whatman GF/F (0.7-µm pore size) filters. For filamentous algae, we used subsamples of wet mass for drying and combustion. For each compartment, we measured algal biomass in terms of ash-free dry mass (AFDM, g m^{-2}) by drying subsamples for 24 h at 60ºC, weighing, then combusting them for 1h at 550 ºC in a muffle furnace and re-weighing. We also measured the algal chlorophyll (chl *a*, mg m^{-2}) using 90% buffered acetone for pigment extraction and spectrophotometric assessment with

acidification following Steinman et al. (2017). We calculated final standing crops for biomass and pigments using corrections for sub-sampling and normalizing results to sampling area.

2.3 Metabolism estimation

Across each of our six sites, we measured dissolved oxygen concentrations using Precision Measurement Engineering (PME) MiniDOT sensors at 5-, 10-, or 15-min intervals from July to October 2020 and June to October 2021. We visited sensors for maintenance and download approximately every two weeks during the sampling periods. We cleaned and linearly interpolated oxygen data to 15-min time steps, correcting irregular time steps and filling in gaps of ≤ 3 h. Oxygen data, including the collection and QA/QC protocol are available in (Valett et al., 2023a).

We estimated reach-scale metabolism using an inverse modeling approach based on sub-daily changes in dissolved oxygen concentrations (Odum, 1956):

$$\frac{dO_2}{dt} = \frac{P_t}{z_t} + \frac{R_t}{z_t} + K_{600,t}(O_{2,sat,t} - O_{2,t}) \quad (1)$$

where $\frac{dO_2}{dt}$ is the change in oxygen concentration each timestep (mg O_2 L^{-1} d^{-1}), P_t is primary production (g O_2 m^{-2} d^{-1}, always positive), R_t is respiration (g O_2 m^{-2} d^{-1}, always negative), z_t is the mean water depth in the upstream reach (m), $K_{600,t}$ is the gas exchange coefficient normalized to a Schmidt number of 600 (d^{-1}), $O_{2,sat,t}$ is the temperature-dependent saturation concentration of oxygen (mg O_2 L^{-1}), and $O_{2,t}$ is the oxygen concentration (mg O_2 L^{-1}), all at time t. We used a Bayesian state-space approach to fit this model in the package *streamMetabolizer* (Appling et al. 2018, v 0.12.0) in R (R Core Team 2022, v 4.2.2). For details on model fitting and QA/QC, see SI text 1 and SI Figures 2, 3. Based on daily estimates of productivity and respiration, we derived net ecosystem production ($NEP = P + R$, g O_2 $m^{-2}d^{-1}$) and the productivity to respiration ratio ($P : R = -P/R$).

2.4 Generalized Additive Models for Algal Biomass

During the 2020 and 2021 growing season, we collected 463 samples representing 11-19 different days at the six sampling sites. We used these data to generate continuous estimates of algal

biomass in the river in order to match biomass measures with extant metabolic estimates. To interpolate algal biomass, we fit generalized additive models (GAMs) to the discrete biomass data. This modeling technique builds flexible regression functions that can describe the relationship between two variables as a smooth curve. In our case, we wanted to use repeated point estimates of algal biomass to predict the biomass as smooth functions of time. These functions allow us to estimate biomass on days without samples.

Because we modeled data from six sites within the same river, we expected that rates and degree of change in biomass to be similar, reflecting an overall shared pattern in response to similar environmental forcing through time. To capture this in a model, we fit a hierarchical GAM that included a global smoother with time (ensuring the same "wiggliness" among sites) as well as a pooled pattern while allowing site to site and year to year deviation from the global function (Pedersen et al., 2019, SI Text 1). We fit the models in R (R Core Team 2022. v 4.2.2) using the mcgv package (Wood, 2017). The hierarchical structure of these models allowed us to aggregate individual sample points into daily estimates without simply taking means and to leverage sites with high data coverage to improve biomass estimates at those with lower coverage. Goodness of fit tests, including QQ plots and residual vs. fitted values plots, indicate that a gamma distribution with a log-link function was a good choice for these data (SI Figure 4) and AIC indicated that a model incorporating both a global and group level smoother was a good fit compared to other model configurations (Pedersen et al., 2019).

2.5 Estimating Biomass Production and Turnover

To relate our metabolism estimates to the building of autotrophic biomass in the stream, we estimated the fraction of each day's P that was immediately respired by autotrophs themselves or by heterotrophs so closely associated with the fixed carbon produced so as to be inseparable from autotrophic respiration. This fraction, referred to as the autotrophic respiration fraction (AR_f), can be estimated by calculating the 90% quantile of the relationship between P and R (Hall and Beaulieu, 2013). This slope represents the fraction of P that is respired within the same day that it was fixed. We calculated the slopes of the 90% quantile for 2020 and 2021 across all six sites

using a multilevel quantile regression in the QRLMM R package (Galarza and Lachos, 2022). In doing so, we pooled across all of the data while still allowing variation across each site year.

Based on our estimates of AR_f, we calculated amount of P that was respired the day it is fixed, which we will call autotrophic respiration (R_A, g O_2 $m^{-2}d^{-1}$) while acknowledging that this number represents both respiration by autotrophs as well as their closely associated heterotrophs (Hall and Beaulieu, 2013), as well as the amount of P that remains as fixed carbon each day, or net production (P_N, g O_2 $m^{-2}d^{-1}$).

$$R_A = P \times AR_f \tag{2}$$

$$P_N = P - R_A \tag{3}$$

We converted fluxes into units of g C $m^{-2}d^{-1}$ by assuming that the photosynthetic quotient (PQ), or the molar ratio of O_2 produced to CO_2 assimilated during photosynthesis, and the respiration quotient (RQ, CO_2 produced to O_2 consumed during respiration) were both equal to 1. We recognize that conditions in the UCFR suggest PQ and RQ probably exceed 1 (Trentman et al., 2023; Shangguan et al., 2024), but this error is small relative to the other parts of this scaling exercise.

Our approach to addressing the linkage between production and biomass embraces epilithic and filamentous morphotypes as representative of distinct autotrophic assemblages in the UCFR. The absolute and relative abundances of these groups differed greatly among sites and between years. To address the interaction between structure and function of the river's autotrophs, we calculated the turnover time (T, d) and the turnover rate (k, d^{-1}) for the entire periphyton as a whole by coupling estimates of P_N and B as:

$$T = \frac{(B_{f,g} + B_{e,g})/2}{P_N} \tag{4}$$

$$k = \frac{1}{T} \tag{5}$$

where filamentous algal biomass ($B_{f,g}$, AFDM) and epilithic algal biomass ($B_{e,g}$, AFDM) were assumed to be 50% carbon by weight.

To parse production between epilithic and filamentous forms, we estimated biomass-specific growth rates per unit light (μ_i/L, g C (mg chl)$^{-1}$ d^{-1}) via a regression approach that coupled P_N to growth rates, algal chlorophyll ($B_{i,chl}$, representative of active algal mass), and available light (L). For light, we used a measure of PAR at the stream surface (μmol m^{-2} d^{-1}) scaled relative to the maximum observed PAR to create a unitless quantity ranging from 0 to 1.

$$P_N = (\mu_f B_{f,chl} + \mu_e B_{e,chl}) \times L \tag{6}$$

Here, each day's net production is partitioned between the filamentous (f) and epilithic (e) algae forms via a zero intercept regression, capturing the assumption that all P_N must come from either B_f or B_e. We used measures of B_i in terms of chlorophyll for this calculation as it represents the metabolically-active fraction of the algal biomass. We calculated the mean rates of biomass production (μ_i) pooled across all sites using a multi-level regression of P_N/L as a function of surrogate biomass estimates (B_f, B_e) which yields global estimates of μ_f and μ_e. We used these estimates to calculate the turnover time (T_i, equation 4) and turnover rate (k_i, equation 5) of each algal form. We estimated algal specific daily production rates (μ_i/L, d^{-1}, Eqn. 7) as the daily net production divided by the standing crop of biomass (g AFDM) of each algal form.

$$\frac{\mu_i}{L} = \frac{P_i}{B_i} \tag{7}$$

We recognize that the metric generated by this approach fails to represent the exact nature of biomass production, standing crops, or turnover times, but argue that it provides an useful comparative measure to assess the interaction between structure and function. Because it relies on empirical data routinely gathered to address periphyton abundance and ecosystem metabolic rates across sites and years, it is a metric that may be widely calculated.

3 Results

3.1 High productivity in the UCFR

The UCFR was highly productive; fluxes of GPP ranged from 0.84 to 21 g O_2 m^{-2} d^{-1} with a mean of 9.2 $\pm$ 0.37 g O_2 m^{-2} d^{-1} (means shown with $\pm$ standard error corrected for autocorrelation (Bence, 1995) throughout results). Productivity tended to peak in the middle of the growing season, late July or August, then decrease into the autumn (Figure 2). Across all sites and both growing seasons, ER was similar to GPP in pattern and magnitude, ranging from -3.2 to -24 g O_2 m^{-2} d^{-1} with a mean of -9.3 $\pm$ 0.46 g O_2 m^{-2} d^{-1}. As a result, daily net ecosystem production (NEP) ranged from -7.7 to 7.2 with seasonal peaks coinciding with productivity, but had a mean near zero (-0.08 $\pm$ 0.19 g O_2 m^{-2} d^{-1}). The correlation between GPP and ER was at least 0.6 for all site years, reaching as high as 0.96 during a bloom year at Bear Gulch. This close association between GPP and ER was reflected in the P:R calculated for each site year, which ranged from 0.69 to 1.19 with a mean of 0.99 $\pm$ 0.014. Half the site years had overall positive NEP and P:R > 1 during the growing season (Figure 2); for five of those six site years, the standard error on the mean of NEP did not include zero (SI Table 1).

3.2 Filamentous algal blooms determined ecosystem structure

Algal standing crop varied among sites and through time, with five of the twelve site-years experiencing a filamentous algae bloom (SI Figure 5). Filamentous algae constituted most of the total algal biomass, ranging from 0 to 170 g AFDM m^{-2} with a mean of 28 $\pm$ 7.4, while epilithic biomass ranged from 1.2 to 43 g AFDM m^{-2} (mean: 11 $\pm$ 1.1 g AFDM m^{-2}). Similarly, the standing crop of chlorophyll *a* was greater in filamentous algae (48 $\pm$ 12 mg chl *a* m^{-2}) than in epilithon (30 $\pm$ 3.0 mg chl *a* m^{-2}). Epilithic and filamentous forms had similar chlorophyll *a* content per unit mass (2.8 $\pm$ 0.3 and 2.8 $\pm$ 0.15 mg g^{-1} respectively). HGAM model fits matched the data well, showing decreased confidence in the estimates when the raw data availability was low (SI Figures 4,5).

Site years with and without algal blooms supported distinctly different filamentous algal

standing crops. Filamentous algae comprised at least 70% in each of the five site years with algal blooms, and made up more than 50% in two of the remaining site years due to correspondingly low epilithon standing crops. The algal assemblage across the 12 site years ranged from those with only epilithic algae to sites with up to 83% filamentous algae (Figure 3). The relative abundance of the two forms of periphyton was not related to metabolic character (i.e., GPP, ER, AR_f, and P_N), but was correlated with both total algal biomass (r = 0.80) and community turnover time (r = 0.77, Figure 3).

Epilithic algal biomass was relatively constant in both space and time; based on modeled interpolations, the epilithon reached a seasonal maximum standing crop of 16 $\pm$ 2.0 g AFDM m^{-2} on average across sites, which was similar to the average standing crop (11 $\pm$ 1.2 g AFDM m^{-2}). The mean (2.4 $\pm$ 0.9 g AFDM m-2) and seasonal maximum (5.2 $\pm$ 1.5 g AFDM m-2) for filamentous algal standing crops were lower across the seven site years without blooms in comparison to bloom conditions when mean (42 $\pm$ 3.1 g AFDM m-2) and seasonal maximums (86 $\pm$ 5.3 g AFDM m-2) were 17- and 16-times greater, respectively (Figure 4a).

3.3 Epilithic algae were more productive than filamentous algae

On a daily time scale GPP was equally partitioned between R_A and biomass production; across sites and years, AR_f ranged from 30 to 65% with a pooled value of 49% (SI Figure 6). Based on estimates from each site year, P_N ranged from 0.93 to 2.4 g C m^{-2} d^{-1} across the twelve site years (mean: 1.7 $\pm$ 0.13 g C m^{-2} d^{-1}).

Epilithic algae cycled rapidly compared to filamentous algae. Partitioning P_N between filamentous and epilithic forms resulted in average C flux values of 1.4 $\pm$ 0.06 g C $m^{-2}d^{-1}$ for epilithic algae and 0.61 $\pm$ 0.24 g C $m^{-2}d^{-1}$ for filamentous algae (SI Figure 7). Over the course of a 100-day growing season, cumulative biomass production by epilithic algae was 136 ± 13 g C m^{-2} (Figure 4a), a value greater than that for filamentous forms both during algal blooms (124 ± 12 g C m^{-2}) and in their absence (7.6 ± 3.7 g C m^{-2}). On average, epilithic algae made up only 32% of the algal standing crop, but were responsible for 69% of the net productivity (SI Figure 7). The emergent effect of the magnitudes of algal biomass and productivity for each of the groups is

manifest as a median turnover time for filamentous forms 4.4 times greater that for epilithic forms (20 and 4.2 d, Figure 4b). These turnover times translate into turnover rates of 0.24 d^{-1} for epilithic algae and 0.05 d^{-1} for filamentous algae.

Regardless of the occurrence of filamentous algal blooms or conditions of net autotrophy, epilithic algae were consistently highly productive compared to filamentous forms. Algal-specific daily production rate (μ_i/L) of epilithic algae ranged from 0.04 to 0.43 d^{-1} (mean: 0.23 $\pm$ 0.01 d^{-1}). In comparison, production rates for filamentous algae ranged from 0.002 to 0.23 d^{-1} with a mean of 0.07 $\pm$ 0.01 d^{-1} calculated from days during which measurable biomass was encountered, a value much lower than that for epilithic forms (Figure 5). The magnitudes and patterns of algal production rates were similar across site-years, regardless of whether it was an autotrophic or heterotrophic growing season, or if there was a filamentous algal bloom (Figure 5). The seasonal pattern in production generally follows autumnal decline in light, with shady days in summer and autumn coinciding with dips in production rate, especially in the epilithic algae (Figure 5).

4 Discussion

The UCFR was highly productive with large summer algal blooms in 5 out of 12 site years. Throughout the river, a relatively constant biomass of epilithic algae covered the rocks while nuisance filamentous algae blooms were heterogeneous in space and time. These blooms greatly changed the total biomass and physical structure of the primary producer assemblage yet the blooms did not appreciably determine rates of gross primary production or ecosystem respiration. Throughout the river, epilithic algae grew and turned over more rapidly than the filamentous algae, accounting for over two thirds of the total production, driving most of the carbon turnover regardless of the presence or absence of slower growing filamentous blooms.

4.1 High biomass and GPP in the Clark Fork

Primary productivity in the UCFR was high compared to most rivers. On average the growing season GPP (Jun-Oct) was higher than 93% of rivers compiled in a recent synthesis (Bernhardt

et al., 2022) and at its peak reached as high as the upper bound suggested for streams that are not light or nutrient limited (Acuña et al., 2011). It was autotrophic during six of the twelve growing seasons in this study, which is uncommon (Bernhardt et al., 2022). Magnitudes of ecosystem respiration closely followed gross primary productivity, suggesting a high degree of autochthony, similar to other western rivers with high light and limited terrestrial carbon inputs (Genzoli and Hall, 2016; Roley et al., 2023).

The algal biomass and successional sequence from mostly epilithic to more filamentous algae followed the same seasonal pattern observed previously in the UCFR (Flynn and Chapra, 2014; Valett et al., 2023b) and in other high nutrient rivers (Suren et al., 2003). Across sites, the algal composition varied primarily due to differences in filamentous algal abundance while epilithic biomass was more constant. At the five site years with filamentous algal blooms, the standing crop of algae qualified as eutrophic, reaching the threshold for nuisance blooms (originally set in the UCFR; Suplee et al. 2012; Dodds et al. 1997). The high rates of productivity and large standing crops of algae can likely be attributed to high light and nutrient availability as well as low frequency of disturbance during the growing season following the snowmelt pulse (Acuña et al., 2011; Bernhardt et al., 2022; Davis et al., 2012). However, it is not clear what triggers a filamentous bloom in some times and places, but not others (Valett et al., 2023b).

4.2 Filamentous algal blooms shaped ecosystem structure, not function

The varying algal assemblage in the UCFR drove patterns in ecosystem structure. Filamentous algal blooms are readily apparent in satellite images (Figure 1) and are the dominant biological feature, apparent to citizens along the UCFR who used visual identification of standing crop to aide in the first riverine chlorophyll water quality standards (Suplee et al., 2009). Unsurprisingly, the fraction of filamentous biomass explained the patterns in total algal biomass. Substantially large standing crops of lotic periphyton are commonly associated with filamentous algal blooms (Davis et al., 2012; Genzoli and Hall, 2016; Blinn et al., 1998). It is likely that the structural effect of filamentous algal blooms extends beyond the autotrophic assemblage. The lower food quality of filamentous algae compared to diatoms (Dodds and Gudder, 1992; Vadeboncoeur and Power,

2017) and thicker algal mats has been observed to decrease macroinvertebrate abundance (Power et al., 2009), and diversity (Tonkin et al., 2014) in other streams. However, whether or not the UCFR experiences any of these structural changes in response to filamentous algal blooms, the shift in algal form was not reflected in the ecosystem metabolic function.

Despite being represented by substantially greater standing crops, filamentous algal blooms did not coincide with enhanced metabolic rates across multiple years and sites. Filamentous algal blooms did not appreciably affect the metabolism or influence whether a stream reach was autotrophic or heterotrophic during a growing season in the UCFR. While algal assemblages varied from almost entirely epilithic to heavily dominated by filamentous forms, metabolic rates (GPP, ER) did not change systematically with form or abundance (Figure 3). Other studies have found that increased algal biomass results in higher productivity both within (Arroita et al., 2019) and across sites (Bernot et al., 2010; Morin et al., 1999; Rodríguez-Castillo et al., 2019). However, many cross site studies find only weak (Bernot et al., 2010; Fellows et al., 2006), or no (Izagirre et al., 2008) relationship between biomass and metabolism. Across a collection of autotrophic sites (i.e., P:R > 1), greater biomass often corresponded to lower productivity (Davis et al., 2012, and references therein), especially in the sites dominated by filamentous algae (Cushing and Wolf, 1984; Mulholland et al., 2001). In the presence of extensive filamentous mats, rates of productivity may be limited, not by external factors such as light and nutrients but by internal dynamics such as space limitation or self-shading by the filamentous algae (Dodds et al., 1999; Kuczynski et al., 2020) or oxygen limitation within the algal mats (Davis et al., 2012).

4.3 Epilithic algae cycled rapidly and drove metabolism

Epilithic biomass standing crops were consistently low, but these algal forms supplied most of the productivity due to rapid growth and turnover. Faster growth of diatom biofilms compared to more structural autotrophic forms such as filamentous algae or macrophytes is well established and has been directly measured in incubations (Arscott et al., 1998) and artificial channels (McIntire, 1973), but these studies are small scale; here we measured algal specific growth rates at the scale of a river reach. The epilithic algae in the UCFR were relatively constant in space and time with

variability in their growth rates mostly tied to changing light conditions. Despite consistently high production, biomass did not accumulate, a condition observed in other systems and attributed to macroinvertebrate grazing (Vadeboncoeur et al., 2021). While no direct assessment of their roles have been made, these dynamics suggest that epilithic algal blooms in the UCFR are limited by availiable substrate and top-down controls in this nutrient-rich river.

The UCFR appears to have environmental conditions favorable for high algal growth rates. Our estimates of algal growth rates were somewhat lower, but of the same order of magnitude as those measured in nutrient-amended mesocosms (Schmidt et al., 2019), and similar to those estimated by early models of simulated streams (McIntire, 1973). On average, the epilithic biofilms in the UCFR turned over every 4-5 d, aligning with estimates made elsewhere (Oemke and Burton, 1986; Cebrian, 1999). Filamentous algae growth rates in the UCFR were well below the maximum rate measured under optimal laboratory conditions (0.77 d^{-1}, Auer and Canale 1982), but it is well known that such high rates are rarely achieved in natural evnironments where self shading or reduction in gas and nutrient exchange can limit growth in dense canopies (Dodds et al., 1999; Choo et al., 2002). Modeled net growth rates of *Cladophora* during the growing season in Lake Erie, an ecosystem known for large filamentous blooms and high phosphorous concentrations, were slightly lower (0 to 0.16 d^{-1}, Higgins et al. 2006) than we observed. This suggests that the growing conditions of high light, high nutrients, and warm water in the UCFR are excellent for algal growth, fostering high production per unit biomass and allowing for turnover of the entire crop more than once per growing season.

4.4 Understanding ecosystem structure and function using metabolism

Simultaneous assessment of algal structure and function is typically limited to isolated cultures or mesocosms (McIntire, 1973; Schmidt et al., 2019). We addressed these dynamics at the scale of stream reaches by pairing reach-scale metabolism with *in situ* measures of algal biomass across multiple reaches of a mid-order river. The result is temporal resolution of the structural and functional character of the autotrophic elements that drive metabolism in a highly productive nutrient-rich river characterized by nuisance blooms of filamentous algae. This approach yielded

realistic growth rates and turnover times of algal groups, providing a means to link temporally resolved functional information with more typical algal biomass measures. This approach could be used to look at seasonal variation in algal growth, understand how primary producers mediate the effect of nutrients or other resources on metabolism, or to model the types of carbon available to aquatic food webs. Approaches that link metabolism time series to algal biomass dynamics demonstrate how the abundance of algal growth forms is reflected in the patterns of primary productivity (Genzoli, 2024). Bridging this gap is needed to enable accurate biomass modeling and prediction from metabolism time series (Blaszczak et al., 2023).

While this method offers valuable insights into algal growth rates, it is limited by its reliance on certain assumptions and the exclusion of key environmental factors, which may affect the accuracy and applicability of the results. To partition productivity, we leveraged the spatial or temporal variability in the algal assemblage; if the fraction of biomass in each group were constant in the dataset, the rates would not be identifiable. We made the simplifying assumption that the biomass specific growth rates of the different algal groups would scale linearly with incident light. This assumption is probably valid for the filamentous fraction of algae, where a more complex physical structure causes self-shading of a portion of the biomass, suggesting that higher light may continue to yield higher production as the light penetrates further into the algal mat's three-dimensional matrix. At high light levels, production may saturate, resulting in lower peak estimates for production than we calculate. Further, this model did not consider other factors such as nutrient availability (Dodds and Gudder, 1992; Stelzer and Lamberti, 2001), temperature (Morin et al., 1999), or invertebrate grazing (Lamberti et al., 1989) in controlling algal growth rates. Any of these mechanisms could be incorporated into future iterations of this approach.

Filamentous algal blooms are a longstanding concern in rivers across diverse landscapes (Biggs and Price, 1987; Genzoli and Hall, 2016; Davis et al., 2012; Oberholster et al., 2017) that may be an increasingly common issue (Vadeboncoeur et al., 2021). Understanding how these blooms affect ecosystem productivity may enable more widespread monitoring of algal dynamics and is a step toward linking filamentous algae to other ecological functions. In the UCFR,

variation in the form of primary producers — epilithic or filamentous — contributed little to the variation in ecosystem productivity. This finding suggests that the shift toward more filamentous biomass may have a similarly small effect on linked elemental cycles such as those for nitrogen and phosphorus. In fact, the filamentous algae blooms in this river have responded minimally to past nutrient reductions (Suplee et al., 2012), possibly due to their lower production rates compared to the epilithic algae. Differences in algal assemblages that drive autotrophic biomass but not system metabolism like we observed in the UCFR may be common in aquatic ecosystems (Genzoli, 2024), representing different associations between structure and function, and a departure from theory for terrestrial ecosystems (Whittaker, 1975; Reichstein et al., 2014).

Acknowledgements

We thank Matt Trentman and Taylor Goldquiros for assistance with depth measurements and Claire Utzman and several students that made collection of biomass samples possible. AMC and ROH were supported by the Modelscapes Consortium with funding from the NSF (OIA-2019528). AMC, RFL, and QS were supported the NSF EPSCoR Track-1 CREWS project (OIA-1757351)

Author Contributions

AMC, ROH, HMV conceived the ideas or experimental design, AMC, ROH, RFL, MD, QS participated actively in the execution of the study, AMC, ROH, RFL analyzed and interpreted the data, AMC wrote the manuscript. All authors contributed edits and approved the final draft.

Conflict of Interest Statement: The authors declare no conflict of interest.

References

Aber, J. D., J. M. Melillo, 2001. Terrestrial Ecosystems. Academic Press, San Diego, CA, second edition.

Acuña, V., C. Vilches, A. Giorgi, 2011. As productive and slow as a stream can be—the metabolism of a pampean stream. *Journal of the North American Benthological Society* **30**:71–83.

Appling, A. P., R. O. Hall, C. B. Yackulic, et al., 2018. Overcoming equifinality: Leveraging long

458 time series for stream metabolism estimation. *Journal of Geophysical Research:*
459 *Biogeosciences* **123**:624–645.
460 Arroita, M., A. Elosegi, R. O. Hall, 2019. Twenty years of daily metabolism show riverine
461 recovery following sewage abatement. *Limnology and Oceanography* **64**:S77–S92.
462 Arscott, D. B., W. B. Bowden, J. C. Finlay, 1998. Comparison of epilithic algal and bryophyte
463 metabolism in an Arctic tundra stream, Alaska. *Journal of the North American Benthological*
464 *Society* **17**:210–227.
465 Auer, M. T., R. P. Canale, 1982. Ecological studies and mathematical modeling of *Cladophora* in
466 Lake Huron: 3. the dependence of growth rates on internal phosphorus pool size. *Journal of*
467 *Great Lakes Research* **8**:93–99.
468 Beaulieu, J. J., C. P. Arango, D. A. Balz, et al., 2013. Continuous monitoring reveals multiple
469 controls on ecosystem metabolism in a suburban stream. *Freshwater Biology* **58**:918–937.
470 Bence, J. R., 1995. Analysis of short time series: correcting for autocorrelation. *Ecology*
471 **76**:628–639.
472 Bernhardt, E. S., P. Savoy, M. J. Vlah, et al., 2022. Light and flow regimes regulate the
473 metabolism of rivers. *Proceedings of the National Academy of Sciences* **119**:5.
474 Bernot, M. J., D. J. Sobota, R. O. Hall, et al., 2010. Inter-regional comparison of land-use effects
475 on stream metabolism. *Freshwater Biology* **55**:1874–1890.
476 Biggs, B. J., G. M. Price, 1987. A survey of filamentous algal proliferations in New Zealand
477 rivers. *New Zealand journal of marine and freshwater research* **21**:175–191.
478 Blaszczak, J. R., C. B. Yackulic, R. K. Shriver, et al., 2023. Models of underlying autotrophic
479 biomass dynamics fit to daily river ecosystem productivity estimates improve understanding of
480 ecosystem disturbance and resilience. *Ecology Letters* **26**:1510–1522.
481 Blinn, D. W., J. P. Shannon, P. L. Benenati, et al., 1998. Algal ecology in tailwater stream
482 communities: the Colorado River below Glen Canyon Dam, Arizona. *Journal of Phycology*
483 **34**:734–740.
484 Cebrian, J., 1999. Patterns in the fate of production in plant communities. *The American*

485 *Naturalist* **154**:449–468.

486 Choo, K.-s., P. Snoeijs, M. Pedersén, 2002. Uptake of inorganic carbon by *Cladophora glomerata*
487 (chlorophyta) from the baltic sea[1]. *Journal of Phycology* **38**:493–502.

488 Cushing, C., E. Wolf, 1984. Primary production in Rattlesnake Springs, a cold desert
489 spring-stream. *Hydrobiologia* **114**:229–236.

490 Davis, C., C. Fritsen, E. Wirthlin, et al., 2012. High rates of primary productivity in a semi-arid
491 tailwater: implications for self-regulated production. *River research and applications*
492 **28**:1820–1829.

493 Del Giorgio, P. A., J. J. Cole, N. F. Caraco, et al., 1999. Linking planktonic biomass and
494 metabolism to net gas fluxes in northern temperate lakes. *Ecology* **80**:1422–1431.

495 Demars, B. O., S. Schneider, K. Thiemer, et al., 2023. Light and temperature controls of aquatic
496 plant photosynthesis downstream of a hydropower plant and the effect of plant removal.
497 *Science of The Total Environment* **912**:169201.

498 Diamond, J. S., F. Moatar, M. J. Cohen, et al., 2022. Metabolic regime shifts and ecosystem state
499 changes are decoupled in a large river. *Limnology and Oceanography* **67**:S54–S70.

500 Dodds, W., V. Smith, B. Zander, 1997. Developing nutrient targets to control benthic chlorophyll
501 levels in streams: a case study of the Clark Fork River. *Water research* **31**:1738–1750.

502 Dodds, W. K., B. J. F. Biggs, R. L. Lowe, 1999. Photosynthesis-Irradiance patterns in benthic
503 microalgae: variations as a function of assemblage thickness and community structure. *Journal*
504 *of Phycology* **35**:42–53.

505 Dodds, W. K., D. A. Gudder, 1992. The ecology of *Cladophora*. *Journal of Phycology*
506 **28**:415–427.

507 Dodds, W. K., E. B. Welch, 2000. Establishing nutrient criteria in streams. *Journal of the North*
508 *American Benthological Society* **19**:186–196.

509 Fellows, C. S., J. E. Clapcott, J. W. Udy, et al., 2006. Benthic metabolism as an indicator of
510 stream ecosystem health. *Hydrobiologia* **572**:71–87.

511 Finlay, J. C., 2001. Stable-carbon-isotope ratios of river biota: implications for energy flow in

lotic food webs. *Ecology* **82**:1052–1064.

Fisher, S. G., G. E. Likens, 1973. Energy flow in Bear Brook, New Hampshire: an integrative approach to stream ecosystem metabolism. *Ecological monographs* **43**:421–439.

Flynn, K. F., S. C. Chapra, 2014. Remote sensing of submerged aquatic vegetation in a shallow non-turbid river using an unmanned aerial vehicle. *Remote Sensing* **6**:12815–12836.

Flynn, K. F., S. C. Chapra, 2020. Evaluating hydraulic habitat suitability of filamentous algae using an unmanned aerial vehicle and acoustic doppler current profiler. *Journal of Environmental Engineering* **146**:04019126.

Furey, P. C., R. L. Lowe, M. E. Power, et al., 2012. Midges, *Cladophora*, and epiphytes: shifting interactions through succession. *Freshwater Science* **31**:93–107.

Galarza, C. E., V. H. Lachos, 2022. qrLMM: Quantile Regression for Linear Mixed-Effects Models. R package version 2.2.

Genzoli, L., 2024. Drivers and fates of primary production in a dammed, eutrophic river. Phd thesis, University of Montana, Missoula, Montana.

Genzoli, L., R. O. Hall, 2016. Shifts in Klamath River metabolism following a reservoir cyanobacterial bloom. *Freshwater Science* **35**:795–809.

Hall, R. O., J. J. Beaulieu, 2013. Estimating autotrophic respiration in streams using daily metabolism data. *Freshwater Science* **32**:507–516.

Higgins, S. N., R. E. Hecky, S. J. Guildford, 2006. Environmental controls of *Cladophora* growth dynamics in eastern lake erie: application of the *Cladophora* growth model (CGM). *Journal of Great Lakes Research* **32**:629–644.

Izagirre, O., U. Agirre, M. Bermejo, et al., 2008. Environmental controls of whole-stream metabolism identified from continuous monitoring of Basque streams. *Journal of the North American Benthological Society* **27**:252–268.

Jankowski, K. J., F. H. Mejia, J. R. Blaszczak, et al., 2021. Aquatic ecosystem metabolism as a tool in environmental management. *WIREs Water* **8**:e1521.

Jassby, A. D., T. Platt, 1976. Mathematical formulation of the relationship between

photosynthesis and light for phytoplankton: Photosynthesis-light equation. *Limnology and Oceanography* **21**:540–547.

Kuczynski, A., A. Bakshi, M. T. Auer, et al., 2020. The canopy effect in filamentous algae: Improved modeling of *Cladophora* growth via a mechanistic representation of self-shading. *Ecological Modelling* **418**:108906.

Lamberti, G. A., S. V. Gregory, L. R. Ashkenas, et al., 1989. Productive capacity of periphyton as a determinant of plant-herbivore interactions in streams. *Ecology* **70**:1840–1856.

McIntire, C. D., 1973. Periphyton dynamics in laboratory streams: a simulation model and its implications. *Ecological Monographs* **43**:399–420.

Minshall, G. W., 1978. Autotrophy in stream ecosystems. *BioScience* **28**:767–771.

Moore, J. N., S. N. Luoma, 1990. Hazardous wastes from large-scale metal extraction. a case study. *Environmental science & technology* **24**:1278–1285.

Morin, A., W. Lamoureux, J. Busnarda, 1999. Empirical models predicting primary productivity from chlorophyll a and water temperature for stream periphyton and lake and ocean phytoplankton. *Journal of the North American Benthological Society* **18**:299–307.

Mulholland, P., A. Steinman, E. Marzolf, et al., 1994. Effect of periphyton biomass on hydraulic characteristics and nutrient cycling in streams. *Oecologia* **98**:40–47.

Mulholland, P. J., C. S. Fellows, J. L. Tank, et al., 2001. Inter-biome comparison of factors controlling stream metabolism. *Freshwater Biology* **46**:1503–1517.

Oberholster, P., V. Somerset, J. Truter, et al., 2017. The interplay between environmental conditions and filamentous algae mat formation in two agricultural influenced South African rivers. *River Research and Applications* **33**:388–402.

Odum, H. T., 1956. Primary production in flowing waters. *Limnology and Oceanography* **1**:102–117.

Odum, H. T., 1957. Primary production measurements in eleven florida springs and a marine turtle-grass community. *Limnology and Ocenography* **2**:85–97.

Oemke, M. P., T. M. Burton, 1986. Diatom colonization dynamics in a lotic system.

Hydrobiologia **139**:153–166.

Patrick, R., 1949. A proposed biological measure of stream conditions, based on a survey of the Conestoga Basin, Lancaster County, Pennsylvania. *Proceedings of the Academy of Natural Sciences of Philadelphia* **101**:277–341.

Pedersen, E. J., D. L. Miller, G. L. Simpson, et al., 2019. Hierarchical generalized additive models in ecology: An introduction with mgcv. *PeerJ* **7**:e6876.

Power, M., R. Lowe, P. Furey, et al., 2009. Algal mats and insect emergence in rivers under mediterranean climates: towards photogrammetric surveillance. *Freshwater Biology* **54**:2101–2115.

R Core Team, 2022. R: A language and environment for Statistical Computing. R Foundation for Statistical Computing.

Reichstein, M., M. Bahn, M. D. Mahecha, et al., 2014. Linking plant and ecosystem functional biogeography. *Proceedings of the National Academy of Sciences* **111**:13697–13702.

Roberts, B. J., P. J. Mulholland, W. R. Hill, 2007. Multiple scales of temporal variability in ecosystem metabolism rates: Results from 2 years of continuous monitoring in a forested headwater stream. *Ecosystems* **10**:588–606.

Rode, M., A. J. Wade, M. J. Cohen, et al., 2016. Sensors in the stream: the high-frequency wave of the present. *Environmental Science and Technology* **50**:10297–10307.

Rodríguez-Castillo, T., E. Estévez, A. M. González-Ferreras, et al., 2019. Estimating ecosystem metabolism to entire river networks. *Ecosystems* **22**:892–911.

Roley, S. S., R. O. Hall Jr, W. Perkins, et al., 2023. Coupled primary production and respiration in a large river contrasts with smaller rivers and streams. *Limnology and Oceanography* **68**:2461–2475.

Rosemond, A. D., 1994. Multiple factors limit seasonal variation in periphyton in a forest stream. *Journal of the North American Benthological Society* **13**:333–344.

Savoy, P., E. Bernhardt, L. Kirk, et al., 2021. A seasonally dynamic model of light at the stream surface. *Freshwater Science* **40**:286–301.

593 Schmidt, T. S., C. P. Konrad, J. L. Miller, et al., 2019. Benthic algal (periphyton) growth rates in
594 response to nitrogen and phosphorus: parameter estimation for water quality models. *JAWRA*
595 *Journal of the American Water Resources Association* **55**:1479–1491.
596 Shangguan, Q., R. A. Payn, R. O. Hall Jr, et al., 2024. Divergent metabolism estimates from
597 dissolved oxygen and inorganic carbon: Implications for river carbon cycling. *Limnology and*
598 *Oceanography* **0**:1–18.
599 Steinman, A. D., G. A. Lamberti, P. R. Leavitt, et al., 2017. Chapter 12 - Biomass and Pigments of
600 Benthic Algae. In F. R. Hauer and G. A. Lamberti, editors, *Methods in Stream Ecology, Volume*
601 *1 (Third Edition)*, pages 223–241. Academic Press, Boston.
602 Stelzer, R. S., G. A. Lamberti, 2001. Effects of N:P ratio and total nutrient concentration on
603 stream periphyton community structure, biomass, and elemental composition. *Limnology and*
604 *Oceanography* **46**:356–367.
605 Stevenson, R. J., M. L. Bothwell, R. L. Lowe, et al., 1996. Algal ecology: Freshwater benthic
606 ecosystem. Academic press.
607 Suplee, M. W., V. Watson, W. K. Dodds, et al., 2012. Response of algal biomass to large-scale
608 nutrient controls in the Clark Fork River, Montana, United States. *JAWRA Journal of the*
609 *American Water Resources Association* **48**:1008–1021.
610 Suplee, M. W., V. Watson, M. Teply, et al., 2009. How green is too green? Public opinion of what
611 constitutes undesirable algae levels in streams. *JAWRA Journal of the American Water*
612 *Resources Association* **45**:123–140.
613 Suren, A. M., B. J. Biggs, C. Kilroy, et al., 2003. Benthic community dynamics during summer
614 low-flows in two rivers of contrasting enrichment. *New Zealand Journal of Marine and*
615 *Freshwater Research* **37**:53–70.
616 Thorp, J. H., M. D. Delong, 2002. Dominance of autochthonous autotrophic carbon in food webs
617 of heterotrophic rivers. *Oikos* **96**:543–550.
618 Tonkin, J. D., R. G. Death, J. Barquín, 2014. Periphyton control on stream invertebrate diversity:
619 is periphyton architecture more important than biomass? *Marine and Freshwater Research*

65:818–829.

Trentman, M. T., R. O. Hall Jr, H. M. Valett, 2023. Exploring the mismatch between the theory and application of photosynthetic quotients in aquatic ecosystems. *Limnology and Oceanography Letters* .

Uehlinger, U., M. W. Naegeli, 1998. Ecosystem metabolism, disturbance, and stability in a prealpine gravel bed river. *Journal of the North American Benthological Society* **17**:165–178.

Vadeboncoeur, Y., M. V. Moore, S. D. Stewart, et al., 2021. Blue waters, green bottoms: Benthic filamentous algal blooms are an emerging threat to clear lakes worldwide. *BioScience* **71**:1011–1027.

Vadeboncoeur, Y., M. E. Power, 2017. Attached algae: the cryptic base of inverted trophic pyramids in freshwaters. *Annual Review of Ecology, Evolution, and Systematics* **48**:255–279.

Valett, H., A. Carter, J. Prater, et al., 2023a. Temperature and concentration of dissolved oxygen in river water measured in the Upper Clark Fork River (Montana, USA) during 2020 and 2021. ver 2. Environmental Data Initiative. https://doi.org/10.6073/pasta/f24a105ec10af98edc7c9314b703e4fc.

Valett, H. M., R. F. de Lima, M. Peipoch, et al., 2023b. Bloom succession and nitrogen dynamics during snowmelt in a mid-order montane river. *Biogeochemistry* **166**:227–246.

Webster, J. R., J. L. Meyer, 1997. Organic matter budgets for streams: A synthesis. *Journal of the North American Benthological Society* **16**:141–161.

Whittaker, R. H., 1975. Communities and ecosystems. Macmillan Publishing Co., New York.

Wood, S., 2017. Generalized Additive Models: An Introduction with R. Chapman and Hall/CRC, second edition.

Figure captions

Figure 1: (a) Satellite image of the Upper Clark Fork River (UCFR) at Bear Gulch taken during a summer algal bloom. (Google, ©2024, Imagery ©2024 Maxar Technologies, USDA/FPAC/GEO) (b) Map of the UCFR showing the locations of metabolism and algal biomass data collection as well as the locations of USGS stream gauges where continuous discharge was measured. Site names are abbreviated as Perkins (PL), Deer Lodge (DL), Garrison (GR), Gold Creek (GC), Bear Gulch (BG), Bonita (BN).

Figure 2: Daily reach-scale metabolism estimates (GPP:green, ER:brown, and NEP:black) across sites during the 2020 and 2021 growing seasons show a mirrored seasonality of GPP and ER with frequent periods of autotrophy (NEP > 0). Site years that were autotrophic for the entire growing season are indicated with 'A' on the panel. Average P:R (mean $\pm$ sd) is provided within each panel. Sites are labeled as in Figure 1.

Figure 3: Across the twelve site-years the algal assemblage (the fraction of algal biomass that is filamentous), does not explain patterns in GPP, ER, the autotrophic respiration fraction, or NPP. Algal assemblage did correlate with the total algal biomass and turnover time. Site years with algae blooms are shown as green triangles. The correlation coefficient (r) is shown on each plot.

Figure 4: (a) Filamentous algae had a greater maximum biomass across sites, especially at sites with algal blooms, but the epilithic algae had higher cumulative production over a 100-d growing season. (b) Epilithic algae turned over rapidly while filamentous turnover times were longer and more variable as shown by the distributions of daily estimates across sites.

Figure 5: Production rate of epilithic algae (blue lines) was high across sites and followed variability in light while filamentous production rate (green lines) was lower and less variable. The patterns were independent of whether a site had a filamentous algae bloom (green areas) or was autotrophic (panels with 'A'). Sites are organized by row and labeled as in Figure 1.

Figures

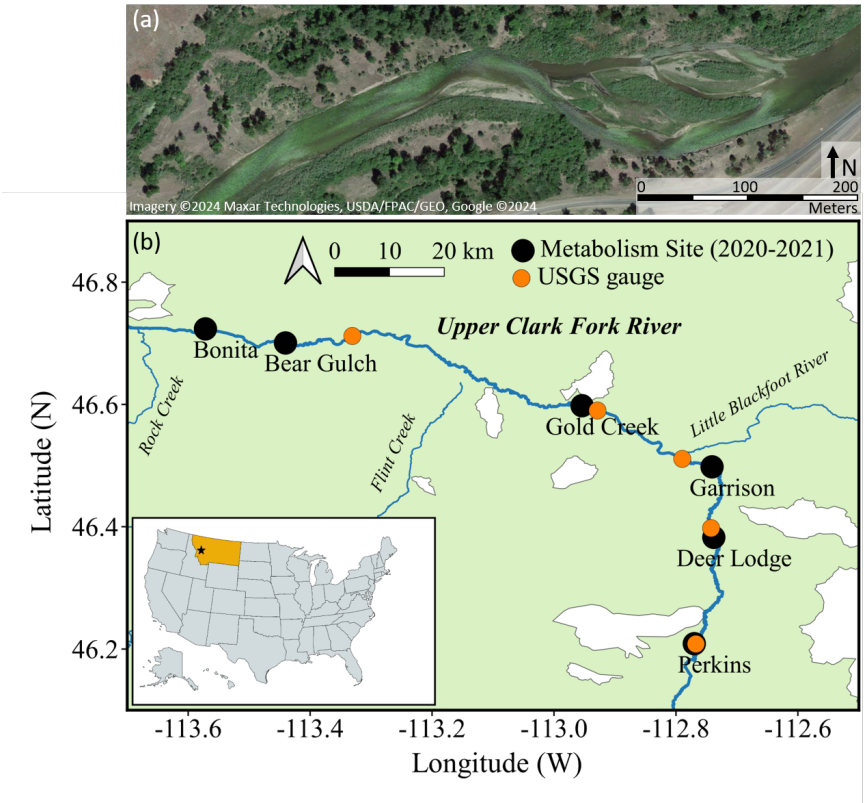

Figure 1:

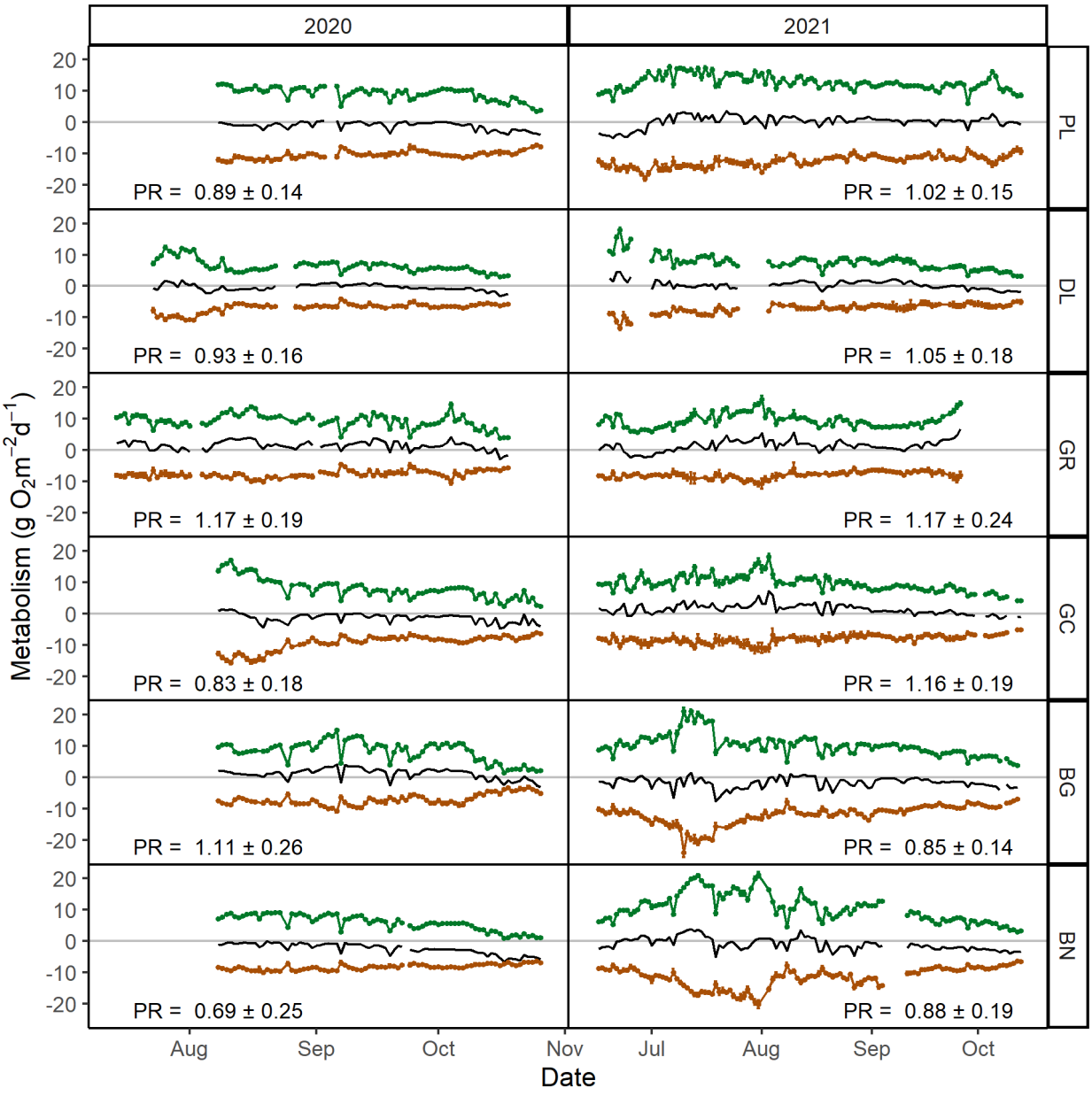
2020
2021
PL
DL
GR
GC
BG
BN
PR = 0.89 ± 0.14
PR = 1.02 ± 0.15
PR = 0.93 ± 0.16
PR = 1.05 ± 0.18
PR = 1.17 ± 0.19
PR = 1.17 ± 0.24
PR = 0.83 ± 0.18
PR = 1.16 ± 0.19
PR = 1.11 ± 0.26
PR = 0.85 ± 0.14
PR = 0.69 ± 0.25
PR = 0.88 ± 0.19
Metabolism (g O2m-2d-1)
20
10
0
-10
-20
Aug
Sep
Oct
Nov
Jul
Aug
Sep
Oct
Date

Figure 2:

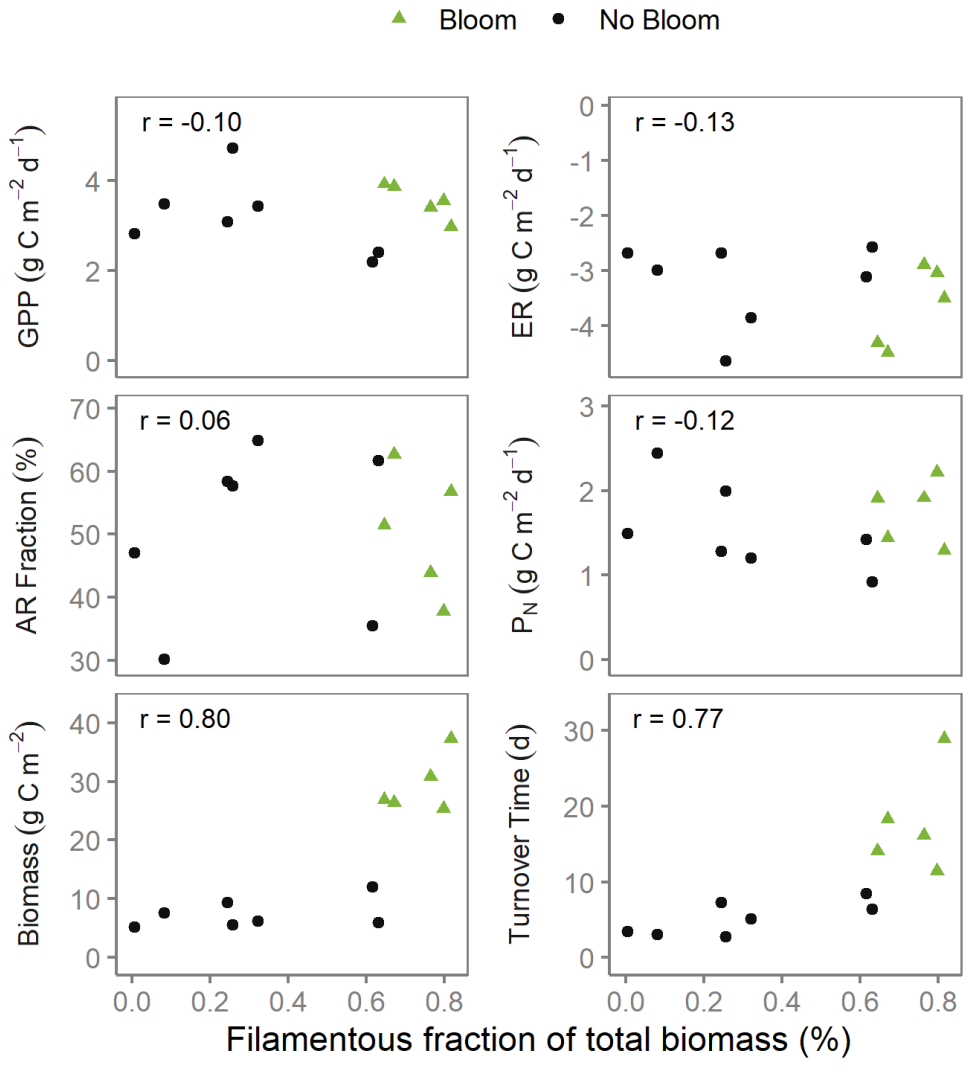
Bloom
No Bloom
r = -0.10
r = -0.13
r = 0.06
r = -0.12
r = 0.80
r = 0.77
GPP (g C m^{-2} d^{-1})
ER (g C m^{-2} d^{-1})
AR Fraction (%)
P_N (g C m^{-2} d^{-1})
Biomass (g C m^{-2})
Turnover Time (d)
Filamentous fraction of total biomass (%)

Figure 3:

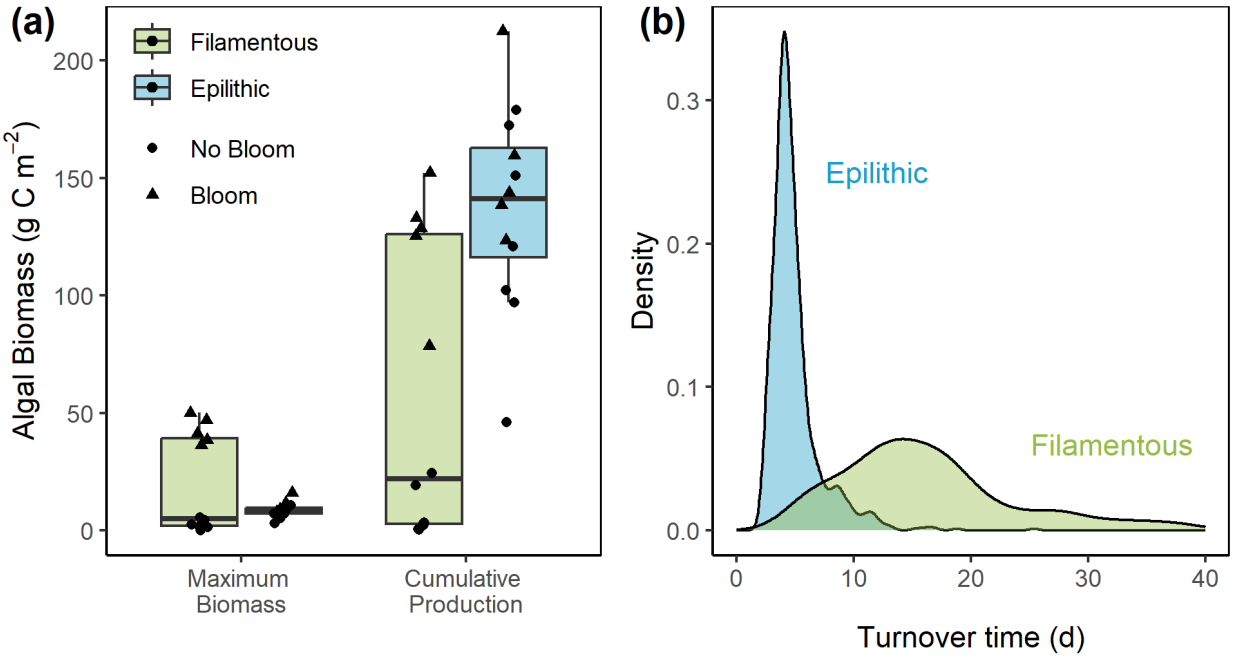
(a)
Filamentous
Epilithic
No Bloom
Bloom
Algal Biomass (g C m^{-2})
200
150
100
50
0
Maximum Biomass
Cumulative Production
(b)
Epilithic
Filamentous
Density
0.3
0.2
0.1
0.0
0
10
20
30
40
Turnover time (d)

Figure 4:

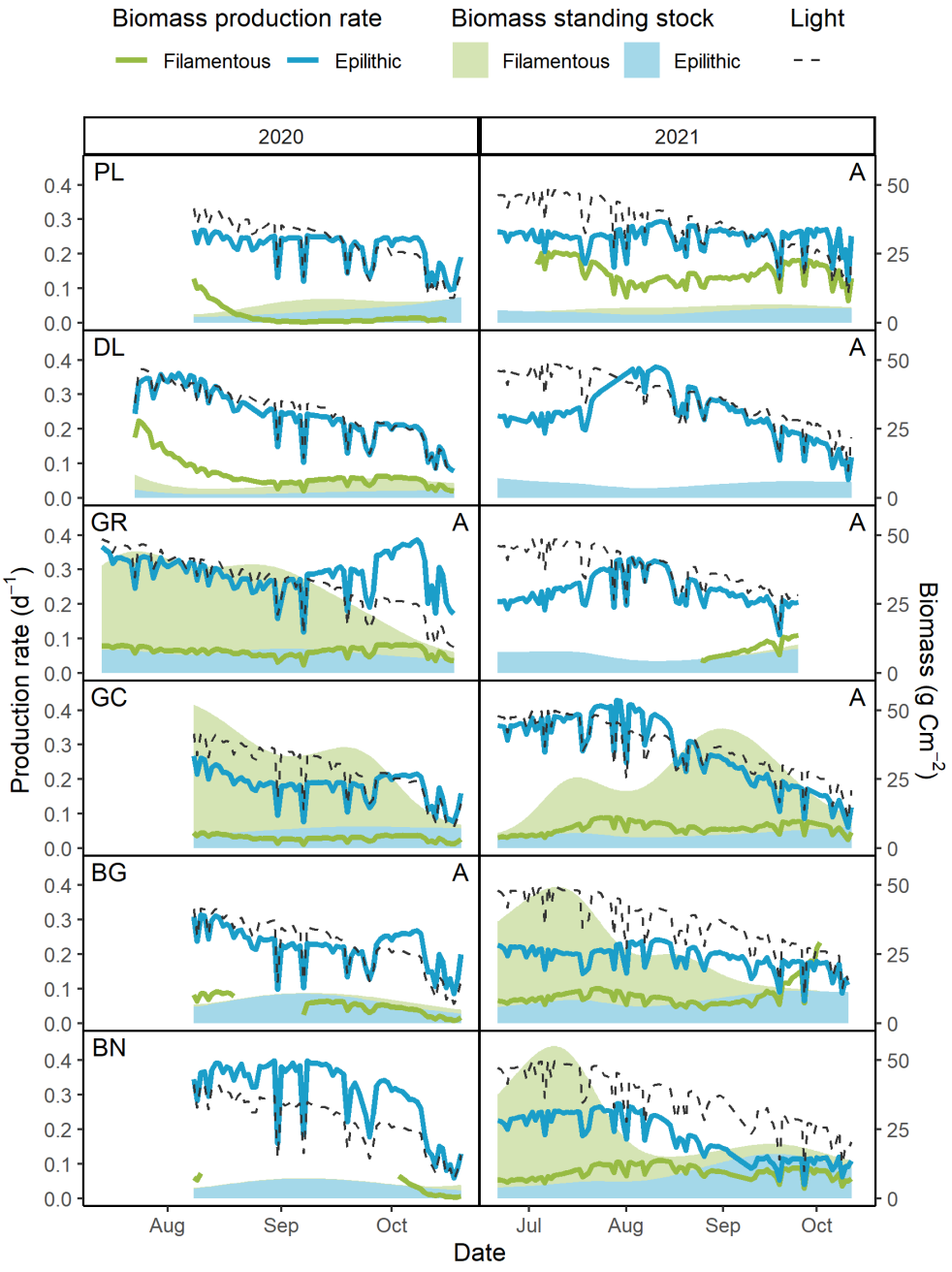
Biomass production rate
Filamentous
Epilithic
Biomass standing stock
Filamentous
Epilithic
Light
2020
2021
PL
DL
GR
GC
BG
BN
A
Production rate (d^{-1})
Biomass (g Cm^{-2})
Aug
Sep
Oct
Jul
Aug
Sep
Oct
Date

Figure 5: